Inorganic Chemistry

Article

pubs.acs.org/IC

Structural Characterization of 2-Imidazolones: Comparison with their Heavier Chalcogen Counterparts

Yi Rong, Ahmed Al-Harbi, Benjamin Kriegel, and Gerard Parkin*

Department of Chemistry, Columbia University, New York, New York 10027, United States

Supporting Information

ABSTRACT: The molecular structures of 1-*t*-butyl-1,3-dihydro-2*H*-imidazol-2-one $[\text{H(oim}^{\text{Bu}^t}\text{)}]$, 1-methyl-1,3-dihydro-2*H*-benzimidazol-2-one $[\text{H(obenzim}^{\text{Me}}\text{)}]$, 1-*t*-butyl-1,3-dihydro-2*H*-benzimidazol-2-one $[\text{H(obenzim}^{\text{Bu}^t}\text{)}]$, and 1-*t*-butyl-1,3-dihydro-2*H*-benzimidazole-2-thione $[\text{H(mbenzim}^{\text{Bu}^t}\text{)}]$ have been determined by single crystal X-ray diffraction. Consideration of the C−O bond lengths in the 2-imidazolones, together with the respective values for 2-thiones and 2-selones, indicates that the C−E bonds in these compounds are intermediate between those of formal C−E single and double bonds, an observation that may be rationalized in terms of a significant contribution of zwitterionic structures that feature single $\text{C}^+{-}\text{E}^-$ dative covalent bonds. In this regard, a natural bond orbital (NBO) analysis of the bonding in $\text{H(}x\text{im}^{\text{Bu}^t}\text{)}$ derivatives demonstrates that a doubly bonded C═E resonance structure is most significant for the oxygen derivative, whereas singly bonded $\text{C}^+{-}\text{E}^-$ resonance structures are dominant for the tellurium derivative, despite the fact that oxygen is more electronegative. The C−E bonding in these compounds is, therefore, significantly different from that in chalcogenoformaldehyde derivatives for which the bonding is well represented by a $\text{H}_2\text{C}{=}\text{E}$ double bonded resonance structure. Comparison of the C−E bond lengths of the imidazolechalcogenones with those of C−E single bonds indicates that the C−O bonds are anomalously short. This observation may be rationalized in terms of the oxygen derivative having not only the most significant π−component but also a substantial ionic component. The latter results from the C−O bond being the most polar due to a substantial polarization of the σ-bond in the direction of oxygen, which thereby supplements the π-polarization and increases the negative charge on oxygen. In contrast, the σ-polarization for the heavier chalcogens opposes the zwitterionic $\text{C}^+{-}\text{E}^-$ π-polarization and thereby reduces the negative charge on the chalcogen. As such, the C−E bond becomes less polar as the chalcogen becomes heavier, despite the fact that the zwitterionic $\text{C}^+{-}\text{E}^-$ contribution increases.

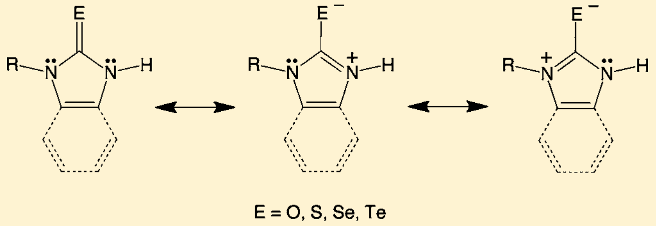

■ INTRODUCTION

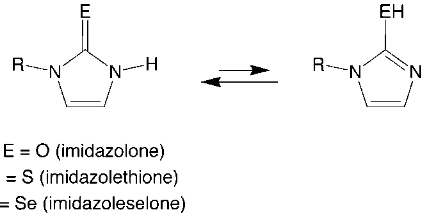

Figure 1. Tautomers of 2-imidazolones, 2-imidazolethiones, and 2-imidazoleselones.

2-Imidazolones,[1] 2-imidazolethiones,[2] and 2-imidazoleselones[3−5] belong to a class of five-membered heterocyclic nitrogen compounds that respectively feature exocyclic C═O, C═S, and C═Se functional groups (Figure 1).[6] In addition to these chalcogenone forms,[7] the molecules also have potential for existing in equilibrium with their chalcogenol tautomers (Figure 1),[8] although the latter are typically less stable.[1−4,9−11] Imidazolones[1,12] and imidazolethiones[2,13] possess various biological activities, with the latter having been most extensively studied because the methyl derivative, methimazole (tapazole), is a widely used antithyroid drug.[13] Imidazoleselones have also received attention with respect to potential antithyroid activity,[3,14] and a derivative has been discovered in the blood of bluefin tuna.[15] 2-Imidazolones,[16] 2-imidazolethiones,[17,18] and 2-imidazoleselones[4b] are also capable of coordinating to metals, and one of our interests pertains to the ability to convert these compounds to multidentate ligands, namely, tris(2-oxoimidazolyl)hydroborato, $[\text{To}^{\text{R}}]$,[19] tris(2-mercaptoimidazolyl)hydroborato, $[\text{Tm}^{\text{R}}]$,[20,21] and *tris*-(2-selenoimidazolyl)hydroborato ligands, $[\text{Tse}^{\text{R}}]$,[21−23] which respectively provide $[\text{O}_3]$, $[\text{S}_3]$, and $[\text{Se}_3]$ donor arrays.[24] By comparison to 2-imidazolethiones, however, relatively few 2-imidazolone compounds have been structurally characterized by X-ray diffraction.[25] Therefore, we report here the molecular structures of 1-*t*-butyl-1,3-dihydro-2*H*-imidazol-2-one $[\text{H(oim}^{\text{Bu}^t}\text{)}]$,[26] 1-methyl-1,3-dihydro-2*H*-benzimidazol-2-one $[\text{H(obenzim}^{\text{Me}}\text{)}]$,[27] and 1-*t*-butyl-1,3-dihydro-2*H*-benzimidazol-2-one $[\text{H(obenzim}^{\text{Bu}^t}\text{)}]$,[28] as illustrated in Figure 2, and

Received: March 30, 2013
Published: June 5, 2013

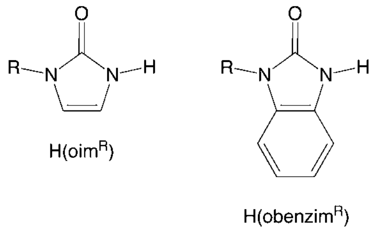

Figure 2. 1-R-imidazol-2-ones (left) and 1-R-benzimidazol-2-ones (right).

compare their structures with the thione and selone counterparts, H(mbenzim$^{\mathrm{Bu^t}}$) and H(sebenzim$^{\mathrm{Bu^t}}$).

■ RESULTS AND DISCUSSION

Structural Comparison of 2-Imidazolone, 2-Imidazolethione and 2-Imidazoleselone Compounds. We have recently described the synthesis and structural characterization of 1-*t*-butyl-1,3-dihydro-2*H*-benzimidazole-2-selone, H(sebenzim$^{\mathrm{Bu^t}}$), thereby demonstrating that the compound exists in the solid state as the selone tautomer and is devoid of intermolecular hydrogen bonding interactions.[4b] While the observation that the compound exists as the selone tautomer is in accord with other derivatives, the absence of intramolecular N−H···Se hydrogen bonding interactions is unexpected on the basis that other 2-imidazoleselones exhibit such interactions.[3d,3g,4a] Furthermore, another interesting feature of H(sebenzim$^{\mathrm{Bu^t}}$) is that the two Se−C−N angles are substantially different [120.7(2)° and 132.1(2)°]. In view of these unusual structural features, it is of interest to compare the structure of H(sebenzim$^{\mathrm{Bu^t}}$) with those of the sulfur and oxygen counterparts, 1-*t*-butyl-1,3-dihydro-2*H*-benzimidazole-2-thione[29] and 1-*t*-butyl-1,3-dihydro-2*H*-benzimidazol-2-one.[26] The molecular structures of H(obenzim$^{\mathrm{Bu^t}}$) and H(mbenzim$^{\mathrm{Bu^t}}$) as determined by X-ray diffraction are, therefore, illustrated in Figures 3 and 4, respectively. In addition, since there are few structurally characterized 2-imidazolone compounds in the literature, the molecular structures of 1-methyl-1,3-dihydro-2*H*-benzimidazol-2-one, H(obenzim$^{\mathrm{Me}}$),[27] and 1-*t*-butyl-1,3-dihydro-2*H*-imidazol-2-one, H(oim$^{\mathrm{Bu^t}}$),[26] are also presented in Figures 5 and 6, respectively. Comparison of the structure of H(oim$^{\mathrm{Bu^t}}$) with that of H(obenzim$^{\mathrm{Bu^t}}$) demonstrates that annulation has little effect on the metrical parameters associated with the [$N_2C{=}O$] moiety (Table 1). Similarly, there is little difference in the [$N_2C{=}S$] moieties of the sulfur derivatives, H(mim$^{\mathrm{Bu^t}}$)[17a] and H(mbenzim$^{\mathrm{Bu^t}}$) (Table 1).

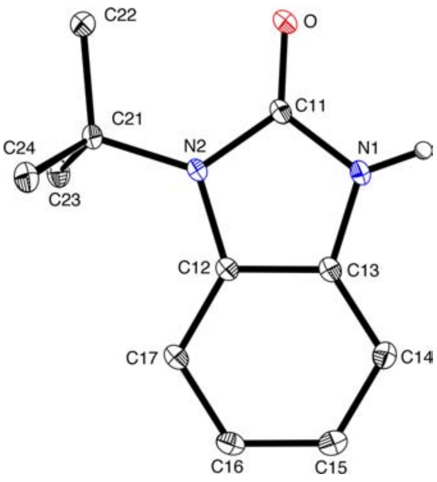

Figure 3. Molecular structure of H(obenzim$^{\mathrm{Bu^t}}$).

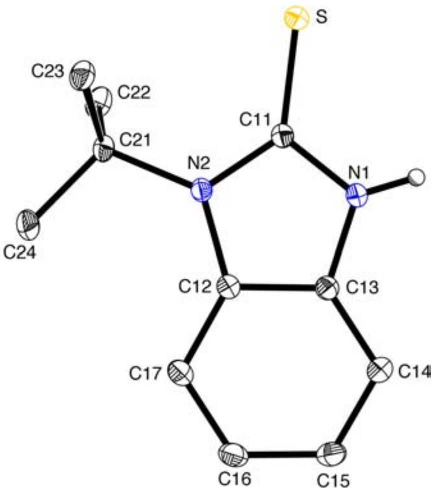

Figure 4. Molecular structure of H(mbenzim$^{\mathrm{Bu^t}}$).

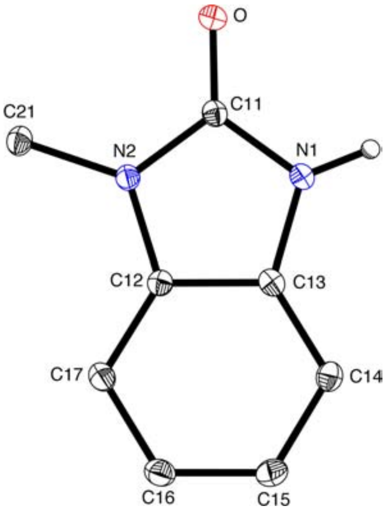

Figure 5. Molecular structure of H(obenzim$^{\mathrm{Me}}$).

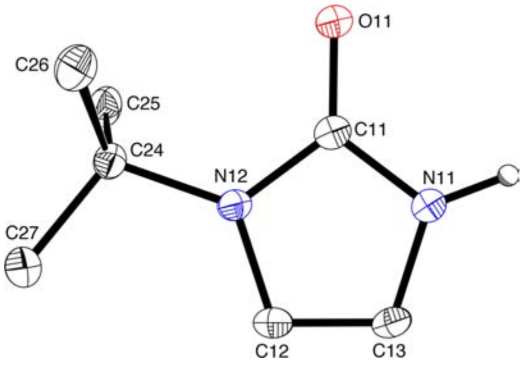

Figure 6. Molecular structure of H(oim$^{\mathrm{Bu^t}}$) (only one of the crystallographically independent molecules is shown).

Examination of Figures 3−6 indicates that each compound exists as its chalcogenone rather than chalcogenol tautomer. While this observation is in accord with other studies pertaining to tautomerism of this class of molecules, the result is noteworthy

Table 1. Metrical Data for 2-Imidazolone, 2-Imidazolethione, and 2-Imidazoleselone Derivatives

	C=E/Å	C–N$_1$/Å^d	C–N$_2$/Å^e	N$_1$–C–E/°^{d}	N$_2$–C–E/°^{e}	Δθ/°^{f}	C–N–C(R)/°	NH···E/Å	N···E/Å	nature of hydrogen bonding interactions
	H(xbenzim$^{Bu^t}$)									
O	1.2372(12)	1.3926(12)	1.3690(12)	127.87(9)	124.95(9)	3.0	127.26(8)	1.88	2.71	dimer
S	1.6851(10)	1.3821(12)	1.3517(12)	130.66(7)	121.83(7)	8.9	123.17(8)	2.50	3.34	dimer
Se^a	1.845(2)	1.370(3)	1.349(3)	132.13(18)	120.69(18)	10.4	122.8(2)	–	–	monomer
	H(xbenzim^{Me})									
O	1.2396(16)	1.3766(17)	1.3719(18)	125.76(13)	127.31(13)	−1.5	124.30(12)	1.90	2.82	dimer
S^b	1.684(2)	1.361(3)	1.356(3)	126.65(17)	126.72(18)	0.0	124.88(18)	2.57	3.41	dimer
Se^a	1.838(2)	1.354(3)	1.356(3)	126.62(17)	126.3(17)	0.3	124.8(2)	2.67	3.48	polymer
	H(xim$^{Bu^t}$)									
O	1.2468(19)	1.368(2)	1.356(2)	127.43(15)	126.35(16)	1.0	124.01(14)	1.80	2.76	dimer
	1.2438(18)	1.373(2)	1.360(2)	127.55(15)	126.56(15)	1.0	123.50(13)	1.853	2.78	
S^c	1.7003(15)	1.3632(18)	1.3484(19)	130.08(11)	123.88(11)	6.2	127.05(12)	2.38	3.27	dimer

[a] Data taken from ref 4b. [b] Data taken from ref 31. [c] Data taken from ref 17a. [d] N$_1$ is the nitrogen atom that is attached to R. [e] N$_2$ is the nitrogen atom that is attached to H. [f] $\Delta\theta$ = [N$_1$–C–E] − [N$_2$–C–E].

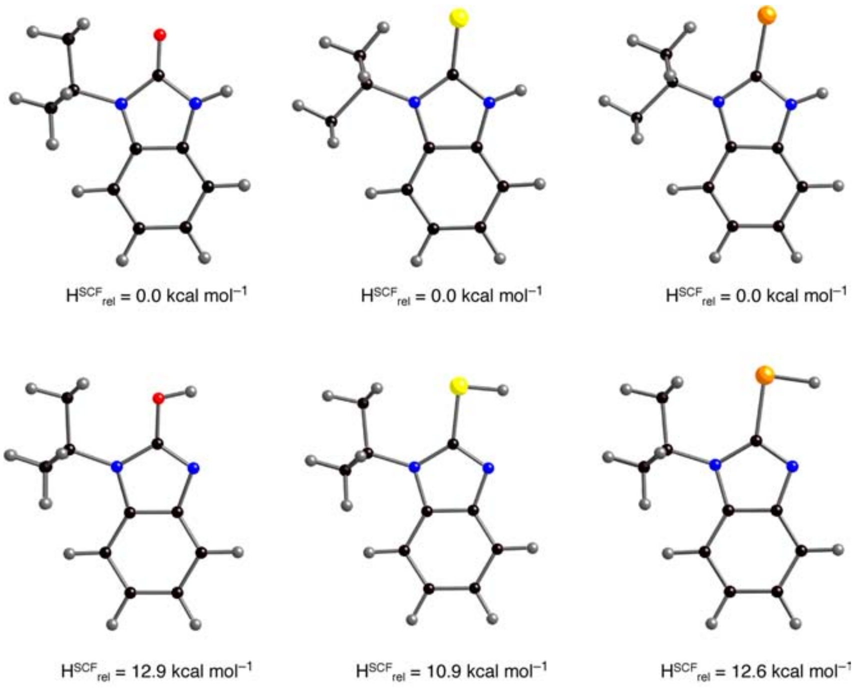

Figure 7. Geometry optimized structures of chalcogenone and chalcogenol tautomers of H(*x*benzim$^{Bu^t}$) (*x* = o, left; m, center; se, right).

in view of the fact that the sulfur derivative H(mbenzim$^{Bu^t}$) has been represented in the literature as existing in the thiol form.[29a] Density functional theory (DFT) calculations, nevertheless, are in accord with the experimental results reported here. Specifically, the chalcogenone tautomers of both H(obenzim$^{Bu^t}$) and H(mbenzim$^{Bu^t}$) are computed to be more stable than their chalcogenol forms (Figure 7 and Table 2). Furthermore, comparison of the H(*x*benzim$^{Bu^t}$) and H(*x*benzim^{Me}) systems (*x* = o, m, se) demonstrates that the chalcogenone tautomer is more favored for the methyl-subsitituted H(*x*benzim^{Me}) system than for the *t*-butyl-substituted H(*x*benzim$^{Bu^t}$) system (Table 2).

With respect to the stabilities of the chalcogenol tautomers, it is pertinent to note that the H(*x*benzim^R) compounds can exist with a variety of different conformations, which differ according to the location of the hydrogen on the chalcogen. In each case, however, the most stable conformation is the one in which the hydrogen on the chalcogen is directed away from the R substituent, i.e., an *exo* location. The preferential adoption of an *exo* conformation is presumably a consequence of steric interactions between the EH and R groups.

Table 2. H_{SCF} Values (kcal mol^{-1}) of Various Conformations of the Chalcogenol Tautomers Relative to That of the Chalcogenone Tautomer

	EH (*exo*)	EH (*endo*)	EH (90°)	EH (*endo*) − EH (*exo*)	H···H distance/Å
H(*x*benzim$^{Bu^t}$)					
O	12.9	21.2	20.4^b	8.3	1.86^c
S	10.9	16.0	15.6^b	5.1	1.96^c
Se	12.6	16.9	16.7^b	4.3	2.03^c
H(*x*benzim^{Me})					
O	14.1	21.6^a	20.7^b	7.5	1.94
S	13.7	16.6^a	15.8^b	2.9	1.95
Se	16.0	17.6^a	17.0^b	0.4	2.01

[a] N–C–E–H torsion angle constrained to 180°. [b] N–C–E–H torsion angle constrained to 90°. [c] Average value for the two close interactions.

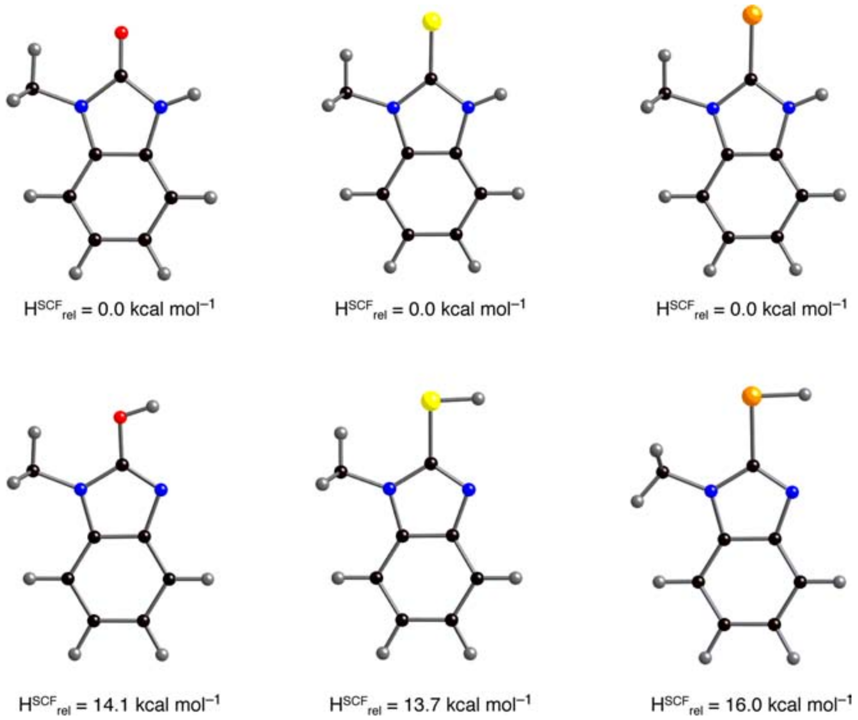

Figure 8. Geometry optimized structures of chalcogenone and chalcogenol tautomers of H(*x*benzim$^{\mathrm{Me}}$) (*x* = o, left; m, center; se, right).

Also of note, the relative stabilities of the *exo* and *endo* conformers depend strongly on the chalcogen, with the *endo* conformer decreasing in stability in the sequence Se > S > O. Supporting the notion that steric interactions play a role in determining the stabilities of the chalcogenol tautomers, the relative energies of the *endo* and *exo* conformers correlate with the shortest nonbonding distance between the chalcogenol hydrogen and the hydrogens of the R substituent within the *endo* conformer. Additional evidence for the importance of steric interactions destabilizing the *endo* isomer is provided by the observation that difference in energies of the *endo* and *exo* conformers is smaller for the methyl-subsitituted H(*x*benzim$^{\mathrm{Me}}$) system than for the *t*-butyl-subsitituted H(*x*benzim$^{\mathrm{Bu^t}}$) system (Figure 8 and Table 2).

The X-ray diffraction studies on H(obenzim$^{\mathrm{Bu^t}}$), H(mbenzim$^{\mathrm{Bu^t}}$) and H(sebenzim$^{\mathrm{Bu^t}}$) also demonstrate that the asymmetry observed in the two N−C−E bond angles of the selenium compound, which differ by 10.4°, is reduced for the sulfur ($\Delta\theta$ = 8.9°) and oxygen ($\Delta\theta$ = 3.0°) counterparts (Table 1). This trend is reproduced by DFT calculations (Figure 7 and Table 3) and is presumably a reflection of steric interactions between the *t*-butyl group and the chalcogen increasing with the size of the chalcogen. In support of this suggestion, the methyl-substituted system, H(*x*benzim$^{\mathrm{Me}}$), exhibits less asymmetry than does the *t*-butyl system H(*x*benzim$^{\mathrm{Bu^t}}$), as illustrated in Figure 8 and Table 3. Thus, whereas $\Delta\theta$ for H(*x*benzim$^{\mathrm{Bu^t}}$) ranges from 4.8° to 14.3°, $\Delta\theta$ for H(*x*benzim$^{\mathrm{Me}}$) only ranges from −0.4° to 3.3° (Table 3).

Table 3. Asymmetry of N−C−E Bond Angles for DFT Geometry Optimized Chalcogenone Isomers of H(*x*benzim$^{\mathrm{R}}$)

	N_1−C−E/°[a]	N_2−C−E/°[b]	$\Delta\theta$/°[c]
H(*x*benzim$^{\mathrm{Bu^t}}$)			
O	129.7	124.9	4.8
S	132.6	121.3	11.3
Se	133.9	119.6	14.3
H(*x*benzim$^{\mathrm{Me}}$)			
O	127.4	127.8	−0.4
S	128.7	126.1	2.6
Se	128.9	125.6	3.3

[a] N_1 is the nitrogen atom that is attached to R. [b] N_2 is the nitrogen atom that is attached to H. [c] $\Delta\theta$ = [N_1−C−E] − [N_2−C−E].

The chalcogenol tautomers of H(*x*benzim$^{\mathrm{Bu^t}}$) also exhibit asymmetry in the two N−C−E bond angles, but the range of $\Delta\theta$ (−1.0° to 10.4°) is smaller than that for the corresponding chalcogenone tautomer (4.8° to 14.3°), as illustrated in Table 4.

Table 4. Asymmetry of N−C−E Bond Angles for DFT Geometry Optimized Chalcogenol Isomers of H(*x*benzim$^{\mathrm{R}}$)

	N_1−C−E/°[a]	N_2−C−E/°[b]	$\Delta\theta$/°[c]
H(*x*benzim$^{\mathrm{Bu^t}}$)			
O	121.5	122.5	−1.0
S	126.9	118.6	8.3
Se	127.9	117.5	10.4
H(*x*benzim$^{\mathrm{Me}}$)			
O	118.5	125.8	−7.3
S	121.2	124.4	−3.2
Se	120.2	125.0	−4.8

[a] N_1 is the nitrogen atom that is attached to R. [b] N_2 is the nitrogen atom that has no substituent. [c] $\Delta\theta$ = [N_1−C−E] − [N_2−C−E].

As expected on the basis of the comparison of the chalcogenone forms of H(*x*benzim$^{\mathrm{Bu^t}}$) and H(*x*benzim$^{\mathrm{Me}}$), the asymmetry for the chalcogenol tautomers of H(*x*benzim$^{\mathrm{Me}}$) is less than that for H(*x*benzim$^{\mathrm{Bu^t}}$).

Examination of the intermolecular interactions (Figures 9−12) demonstrates that all of the 2-imidazolone compounds exist as hydrogen bonded dimers, as does the 2-imidazolethione derivative, H(mbenzim$^{\mathrm{Bu^t}}$). Thus, the N···O distances of H(obenzim$^{\mathrm{Bu^t}}$) [2.7873(11) Å], H(obenzim$^{\mathrm{Me}}$) [2.8214(16) Å],

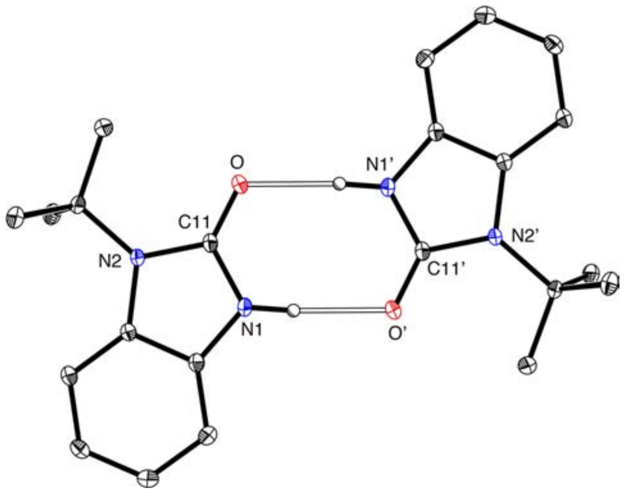

Figure 9. Hydrogen bonded dimeric structure of H(obenzim$^{\mathrm{Bu^t}}$). Hydrogen bonding distance: d(N1···O′) = 2.7873(11) Å.

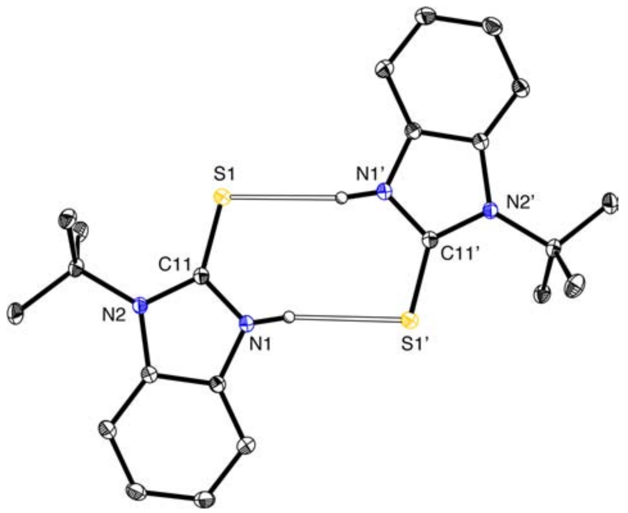

Figure 10. Hydrogen bonded dimeric structure of H(mbenzim$^{\mathrm{Bu^t}}$). Hydrogen bonding distance: d(N1···S1′) = 3.3422(9) Å.

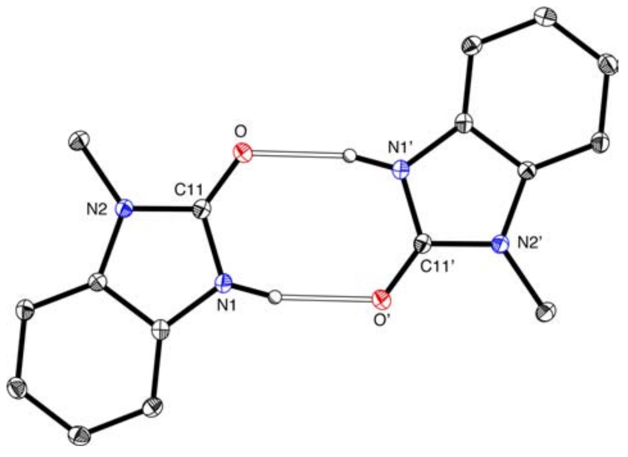

Figure 11. Hydrogen bonded dimeric structure of H(obenzim$^{\mathrm{Me}}$). Hydrogen bonding distance: d(N1···O′) = 2.8214(16) Å.

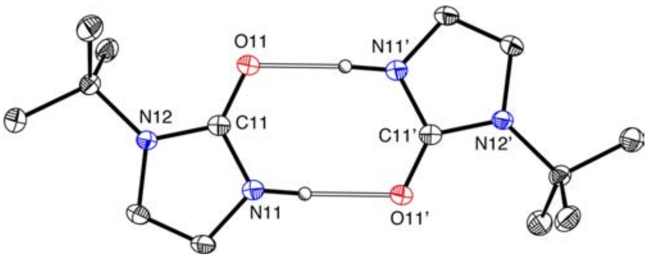

Figure 12. Hydrogen bonded dimeric structure of H(oim$^{\mathrm{Bu^t}}$) (only one of the crystallographically independent molecules is shown). Hydrogen bonding distances: d(N11···O11′) = 2.7581(19) Å; d(N21···O21′) = 2.7798(18) Å.

and H(obenzim$^{\mathrm{Bu^t}}$) [2.7581(19) Å and 2.7798(18) Å], and the N···S distance of H(mbenzim$^{\mathrm{Bu^t}}$) [3.3422(9) Å], are in the range typical of N–H···O and N–H···S hydrogen bonding interactions.[30] In this regard, the hydrogen bonded structures of H(obenzim$^{\mathrm{Bu^t}}$) and H(mbenzim$^{\mathrm{Bu^t}}$) are in marked contrast to that of the selenium counterpart, H(sebenzim$^{\mathrm{Bu^t}}$), which does not participate in hydrogen bonding interactions.[4b] Also of interest, the dimeric structure of the methylbenzimidazolone compound, H(obenzim$^{\mathrm{Me}}$), is distinct from those of both the mercapto[31] and seleno[4b] counterparts which possess polymeric "head-to-tail" structures. It is, therefore, evident that both the nature of the chalcogen and the 1–R substituent exert an influence on the hydrogen bonding motif of these compounds.

Electronic Structure of the Chalcogenone Compounds. The variation in the C═E bond lengths for the chalcogenone compounds, H(oim$^{\mathrm{Bu^t}}$) and H($x$benzim$^{\mathrm{R}}$), is summarized in Figure 13. For comparison, Figure 13 also includes the average C–E single bond length data for compounds that are listed in the Cambridge Structural Database (CSD),[32] together with the bond lengths for X_2C═E compounds. These data indicate that the C–E bonds in these chalcogenones are 0.017–0.029 Å longer

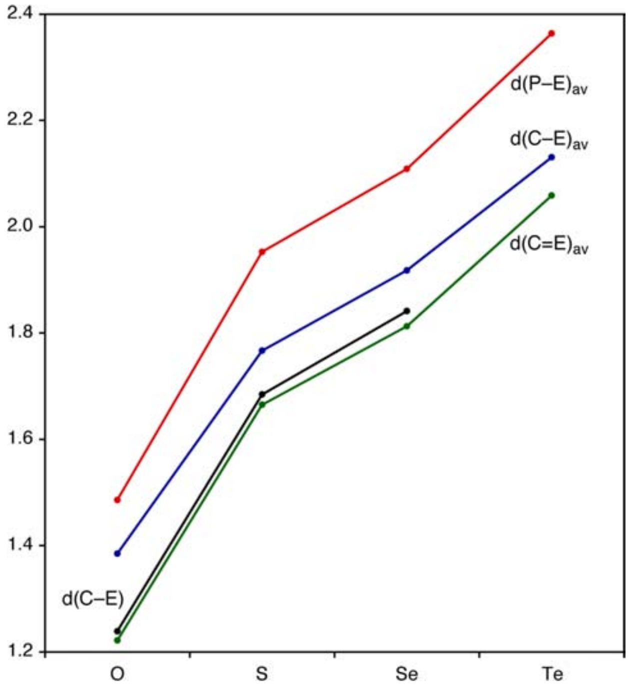

Figure 13. Variation of average C–E bond lengths in H(oim$^{\mathrm{Bu^t}}$) and H($x$benzim$^{\mathrm{R}}$) (black line). For comparison, CSD average data for C–E single and double bonds, together with P–E data for R_3PE compounds, are also included.

than the CSD average for other $X_2C{=}E$ compounds, in accord with the notion that zwitterionic structures, which feature single $C^+{-}E^-$ dative covalent bonds,[33] provide an important contribution in such molecules (Figure 14).[34]

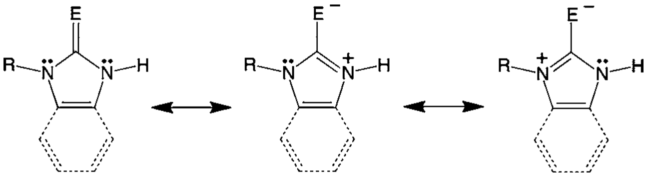

Figure 14. Three principal resonance structures for 2-imidazolechalcogenones. Other resonance structures also exist.

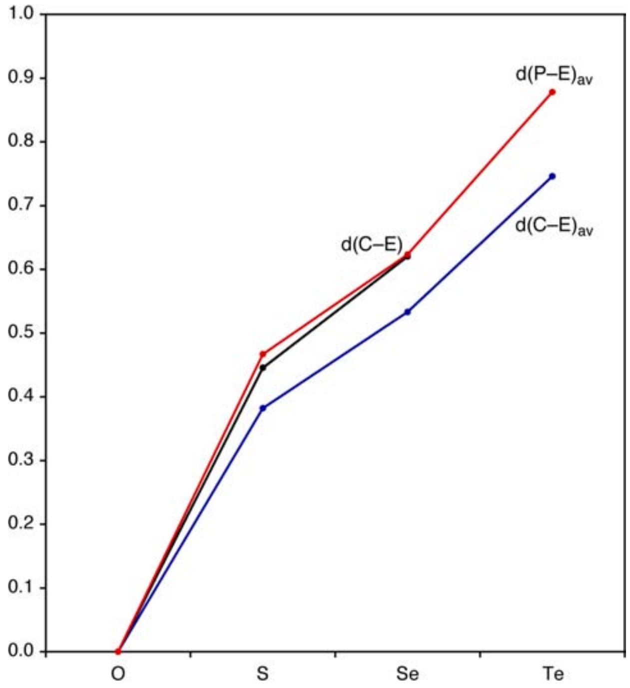

Figure 15. Variation of average C–E bond lengths in H(oim$^{\mathrm{Bu^t}}$) and H(*x*benzim$^{\mathrm{R}}$), normalized to the C–O bond length (black line). For comparison, analogous data for CSD average data for C–E single bonds, together with P–E data for R_3PE compounds, are also included. Note that the C–S and C–Se bond lengths in H(*x*benzim$^{\mathrm{R}}$) are longer than would be expected if the trend were to follow the variation in C–E single bond lengths (blue line); correspondingly, the C–O bond lengths in H(oim$^{\mathrm{Bu^t}}$) and H(*x*benzim$^{\mathrm{R}}$) are shorter than would be anticipated.

Further insight into the nature of the C–E interactions within these chalcogenones is provided by analysis of the difference between the observed C–E bond lengths and the CSD average C–E single bond lengths as a function of the chalcogen (Table 5). Examination of these data indicate that the difference between the observed C–E bond lengths of the chalcogenones and the corresponding C–E single bond lengths is greatest for the oxygen derivative. Another illustration of the differences is provided by the variation of C–E bond lengths that have been normalized to the value for the oxygen derivative (Figure 15). Specifically, the C–E bonds in the chalcogenones do not parallel the changes in CSD average C–E single bond lengths. Thus, relative to the oxygen derivative, the C–S and C–Se bonds of the chalcogenone compounds are longer than expected; conversely, the C–O bonds may be viewed as being anomalously short.

While one explanation for the exceptionally short C–O bond length could be that the oxo compound possesses a greater contribution of the doubly bonded resonance structure (Figure 14), the observation that R_3PE compounds also exhibit anomalously short P–O bond lengths indicates that such an argument is overly simplistic. Specifically, since it is well-known that R_3PE is better represented as possessing a $P^+{-}E^-$ zwitterionic interaction rather than a $P{=}E$ double bond (which would be associated with an expanded octet),[35] the unusually short P–O bond in R_3PO derivatives cannot be rationalized in terms of a multiple covalent bond. Therefore, the short C–O bond length in the imidazolone compounds may not solely be a consequence of a doubly bonded $C{=}O$ resonance structure, but may also reflect an ionic component to the bonding.[36]

To address this issue, the bonding in the chalcogenones has been evaluated by using natural bond orbital (NBO) methods.[35,37] In this regard, while analysis of the natural localized molecular orbitals (NLMO's) indicates that the amount of π–overlap is most significant for the oxygen derivative, the polarization of the C–E bond is also the greatest for the oxygen derivative (Table 6 and Figure 16). Thus, the combination of a substantial π-component and an ionic component to the bonding results in an exceptionally short C–O bond relative to the C–S bond.

It is also worth contrasting the bonding in H(*x*im$^{\mathrm{Bu^t}}$) with those of the formaldehyde derivatives, H_2CE. Thus, whereas the π-bonds of H(*x*im$^{\mathrm{Bu^t}}$) become progressively localized on the chalcogen in the sequence O < S < Se < Te (i.e., approaching a lone pair orbital for the latter),[38] the π-bonds for H_2CE retain a significant contribution from carbon (36–46%) for all of the chalcogen derivatives (Table 7).[39] Another interesting difference between H(*x*im$^{\mathrm{Bu^t}}$) and H_2CE is that the two series of compounds have opposite polarizations for the C–S, C–Se, and C–Te bonds; i.e., the chalcogens are negative for H(*x*im$^{\mathrm{Bu^t}}$) but positive for H_2CE (Table 7 and Figure 17). A rationalization for this difference in polarization is provided by consideration of the σ and π ionicities, $(c_C^2 - c_E^2)/(c_C^2 + c_E^2)$, where c_X is the NBO polarization coefficient for atom X. Specifically, whereas the σ ionicities for both H(*x*im$^{\mathrm{Bu^t}}$) and H_2CE vary in a manner that reflect differences in electronegativity, i.e., the chalcogen becomes less negative in the sequence O > S > Se > Te (Figure 18), the π ionicities vary in such a manner that the chalcogen becomes less negative for H_2CE, but more negative for H(*x*im$^{\mathrm{Bu^t}}$), as illustrated in Figure 18.[40] The latter is a consequence of zwitterionic structures (Figure 14) being more dominant for the heavier chalcogen derivatives of H(*x*im$^{\mathrm{Bu^t}}$), thereby resulting in a polarization that opposes simple electronegativity considerations. In this

Table 5. Comparison of C–E Bond Lengths in H(oim$^{\mathrm{Bu^t}}$) and H(*x*benzim$^{\mathrm{R}}$) with CSD Mean C–E Single and Double Bonds

	d(C–E)/Å^a	CSD mean single bond d(C–E)/Å	CSD mean double bond d(C=E)/Å	d(C–E)/Å – d(C–E)/Å
O	1.239	1.385	1.222	0.146
S	1.685	1.767	1.665	0.082
Se	1.842	1.918	1.813	0.076

^{a}Average value for H(oim$^{\mathrm{Bu^t}}$) and H(*x*benzim$^{\mathrm{R}}$) derivatives.

Table 6. NLMO Composition, Atomic Charges (Q), and Ionicities (i_{CE})^{a} for C−E Moieties of H($x$im$^{Bu^t}$)

	σ-orbital		π-orbital							
	$\sigma_{\%C}$	$\sigma_{\%E}$	$\pi_{\%C}$	$\pi_{\%E}$	Q_C/e	Q_E/e	Q_E-Q_C/e	$i_{CE}(\sigma)$	$i_{CE}(\pi)$	$i_{CE}(\sigma) + i_{CE}(\pi)$
O	35.8	64.0	26.8	73.0	0.79	−0.68	−1.47	−0.28	−0.46	−0.74
S	60.0	39.2	24.8	74.8	0.22	−0.30	−0.52	0.21	−0.50	−0.29
Se	65.5	33.5	13.1	82.4	0.16	−0.26	−0.42	0.32	−1.00^{b}	−0.68
Te	71.3	27.4	7.1	87.9	0.10	−0.23	−0.33	0.45	−1.00^{b}	−0.55

$^{a}i_{CE} = (c_C^2 - c_E^2)/(c_C^2 + c_E^2)$, where c_X is the NBO polarization coefficient for atom X. A negative value of i_{CE} indicates that the chalcogen atom possesses a negative charge. Values listed are calculated for the dominant resonance structures. $^{b}i_{CE}(\pi)$ is assigned a value of −1 because the NBO is localized on the chalcogen atom.

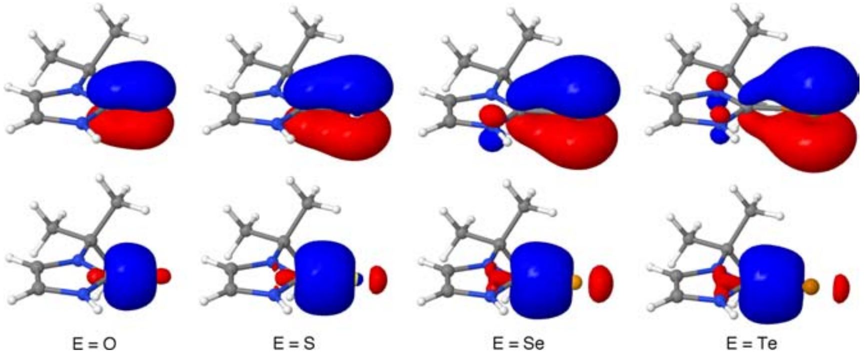

Figure 16. σ and π−NLMOs for H($x$im$^{Bu^t}$).

Table 7. NLMO Composition, Atomic Charges (Q), and Ionicities (i_{CE})^{a} for C−E Moieties of H_2CE

	σ-orbital		π-orbital							
	$\sigma_{\%C}$	$\sigma_{\%E}$	$\pi_{\%C}$	$\pi_{\%E}$	Q_C/e	Q_E/e	Q_E-Q_C/e	$i_{CE}(\sigma)$	$i_{CE}(\pi)$	$i_{CE}(\sigma) + i_{CE}(\pi)$
O	33.7	66.3	35.6	64.4	0.22	−0.49	−0.71	−0.33	−0.29	−0.62
S	56.1	43.9	44.0	56.0	−0.52	0.08	0.60	0.12	−0.12	0.00
Se	61.1	38.9	45.1	54.9	−0.65	0.18	0.83	0.22	−0.10	0.12
Te	66.5	33.5	46.2	53.8	−0.77	0.30	1.07	0.33	−0.08	0.25

$^{a}i_{CE} = (c_C^2 - c_E^2)/(c_C^2 + c_E^2)$, where c_X is the NBO polarization coefficient for atom X. A negative value of i_{CE} indicates that the chalcogen atom possesses a negative charge. Values listed are calculated for the dominant resonance structures.

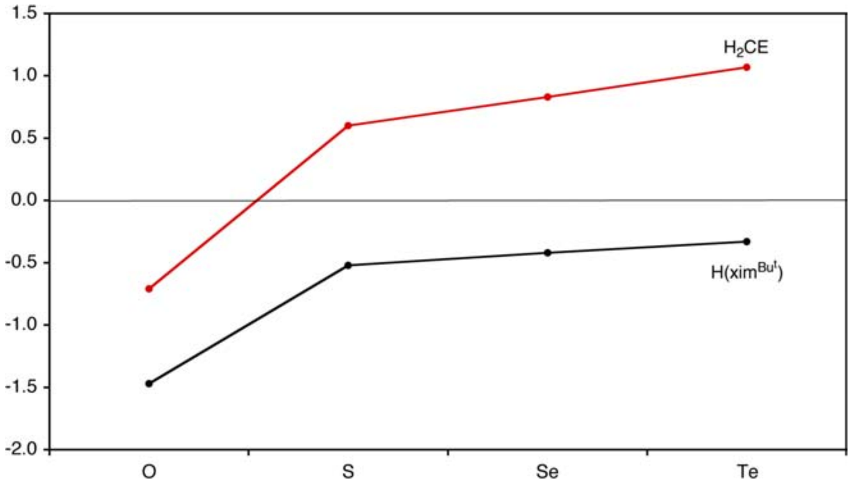

Figure 17. Polarization of the C−E bonds in H($x$im$^{Bu^t}$) and H_2CE as expressed by Q_E-Q_C. Note that the chalcogen is negatively charged for all of the H($x$im$^{Bu^t}$) series, whereas only the oxygen atom is negatively charged for the H_2CE series.

regard, it is important to note that electronegativity, as expressed in the context of NBO theory, is an orbital property, such that the σ- and π-electronegativities of an atom are not required to have the same value.[35] As an illustration of this issue, despite the fact that zwitterionic C^+-E^- resonance structures[33] are most dominant for the tellurium derivative, the most negatively charged chalcogen within the H($x$im$^{Bu^t}$) series is that of the oxygen derivative due to the ionicity associated with the σ-bonding.

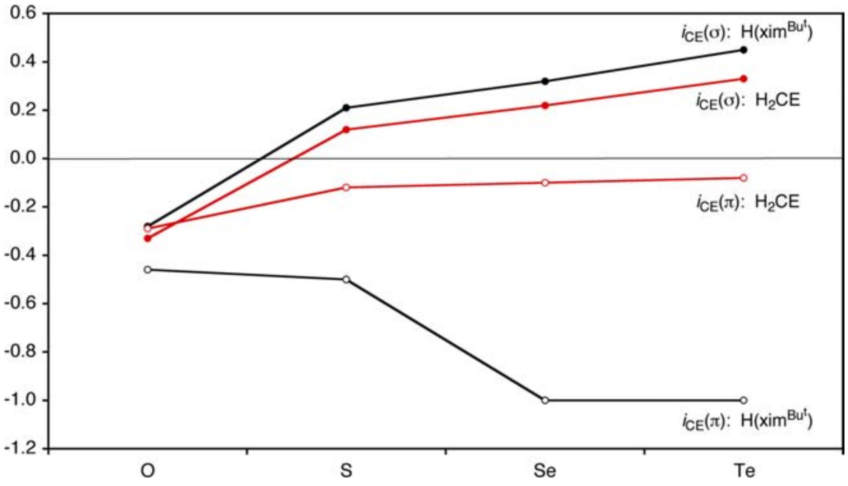

Figure 18. σ- and π-components of the ionicity of the C−E bonds in the dominant resonance structures of H($x$im$^{\mathrm{Bu^t}}$) and H_2CE (Tables 8 and 9), as expressed in a form in which the sign of i_{CE} refers to the charge on the chalcogen. Note that the σ components of H($x$im$^{\mathrm{Bu^t}}$) and H_2CE result in a less negative charge for the heavier chalcogens and are actually positive for sulfur, selenium, and tellurium derivatives. While the π components are all negative, the two series of compounds exhibit opposing trends, with the charge on the chalcogen becoming less negative for the heavier chalcogens in the H_2CE series, but more negative in the H($x$im$^{\mathrm{Bu^t}}$) series. The latter trend is in accord with an increased contribution from the zwitterionic C^+−E^-resonance structure for the heavier chalcogen derivatives of H($x$im$^{\mathrm{Bu^t}}$).

Table 8. Principal Resonance Structures for H($x$im$^{\mathrm{Bu^t}}$) and Their Contribution (%), Together with the Total Contributions of Resonance Structures with C−E Single and C═E Double Bonds

	O	S	Se	Te
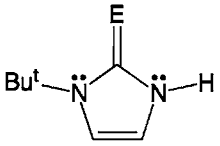	32.60*	25.32*	21.30	16.48
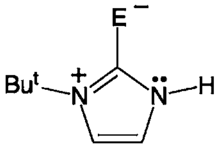	16.20	20.78	21.76*	23.60*
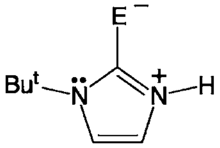	14.78	17.33	20.37	22.87
Total contribution of resonance structures with C=E double bonds	47.74	36.23	29.99	21.11
Total contribution of resonance structures with C–E single bonds	43.95	58.38	63.51	72.16

*Dominant resonance structure.

Table 9. Principal Resonance Structures for H_2CE and Their Contribution (%)

	O	S	Se	Te
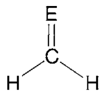	94.23*	96.40*	97.30*	98.07*
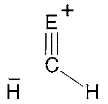	2.88	1.80	1.35	0.96
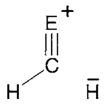	2.88	1.80	1.35	0.96

*Dominant resonance structure.

The principal resonance structures for H($x$im$^{\mathrm{Bu^t}}$) are summarized in Table 8, which reveals several noteworthy features. First, the total contribution of doubly bonded C═E resonance structures for H($x$im$^{\mathrm{Bu^t}}$) (47.7% for E = O to 21.1% for E = Te) is much less significant than the corresponding forms for both H_2CE (94.2% for E = O to 98.1% for E = Te; Table 9) and $H_2NC(E)H$ (58.6% for E = O to 56.1% for E = Te).[41] Second, the combined zwitterionic resonance structures with C−E single bonds for H($x$im$^{\mathrm{Bu^t}}$) become relatively more important in the sequence O < S < Se < Te, and are the dominant resonance structures for the sulfur, selenium, and tellurium derivatives.[42] While this result may appear counterintuitive because it is opposite to the trend that one would expect on the basis of electronegativity differences, similar observations have been made for (i) urea, thiourea, and selenourea derivatives, and also (ii) formamide, thioformamide, selenoformamide, telluroformamide, and related derivatives.[41,43−48] For example, $n_N \rightarrow \pi^*_{C-E}$ delocalization was observed to increase in the sequence O < S < Se, whereas the atomic charges and polarization of the C−E bond decrease in the sequence O > S > Se.[43] As such, it has been suggested that orbital interactions rather than electronegativities play the more important role in determining the electron delocalization.[43] Orbital interactions are more favorable for the heavier chalcogen derivative because the antibonding π^*_{C-E} orbital is lower in energy and so it serves as a better acceptor for the nitrogen lone pair.[43,49] In contrast to H($x$im$^{\mathrm{Bu^t}}$) and $XC(E)NH_2$ derivatives, the C−E bonds of

Table 10. Crystal, Intensity Collection, and Refinement Data

	H(obenzim$^{Bu^t}$)	H(mbenzim$^{Bu^t}$)	H(obenzim^{Me})	H(oim$^{Bu^t}$)
lattice	monoclinic	monoclinic	monoclinic	monoclinic
formula	$C_{11}H_{14}N_2O$	$C_{11}H_{14}N_2S$	$C_8H_8N_2O$	$C_7H_{12}N_2O$
formula weight	190.24	206.3	148.16	140.19
space group	$P2_1/n$	$P2_1/c$	$P2_1/n$	$P2_1/c$
a/Å	11.2515(19)	7.7333(5)	9.2105(16)	12.0988(17)
b/Å	7.9498(14)	16.9079(10)	5.5849(10)	10.6355 (15)
c/Å	11.536(2)	8.4588(5)	13.456(2)	12.0130(17)
α/°	90	90	90	90
β/°	106.507(2)	106.2250(10)	91.481(2)	94.073(2)
γ/°	90	90	90	90
V/Å^3	989.3(3)	1061.97(11)	707.0(2)	1541.9(4)
Z	4	4	4	8
temperature (K)	125(2)	150(2)	125(2)	130(2)
radiation (λ, Å)	0.71073	0.71073	0.71073	0.71073
ρ (calcd.), g cm^{-3}	1.277	1.290	1.392	1.208
μ (Mo Kα), mm^{-1}	0.084	0.266	0.095	0.083
θ max, deg	29.57	32.66	30.69	30.76
no. of data collected	14457	18173	10956	24556
no. of data used	2766	3753	2181	4784
no. of parameters	134	130	105	195
R_1 [$I > 2\sigma(I)$]	0.0392	0.0375	0.0478	0.0572
wR_2 [$I > 2\sigma(I)$]	0.1090	0.0983	0.1057	0.1059
R_1 [all data]	0.0463	0.0447	0.0752	0.1271
wR_2 [all data]	0.1154	0.1033	0.1183	0.1287
GOF	1.063	1.047	1.040	1.012

chalcogenoformaldehyde compounds, H_2CE, in which there is no adjacent nitrogen substituent with a lone pair, have little zwitterionic character (Table 9). In fact, the most dominant (albeit small) zwitterionic component of H_2CE possesses a $C^-{\equiv}E^+$ triple bond, such that the polarization is actually the opposite of those of H(*x*im$^{Bu^t}$) and XC(E)NH_2.

■ SUMMARY

In conclusion, the C−E bond lengths of 2-imidazolone, 2-imidazolethione, and 2-imidazoleselone compounds are intermediate between those of formal C−E single and double bonds, an observation that is in accord with the notion that zwitterionic structures that feature single $C^+{-}E^-$ dative covalent bonds provide an important contribution in such molecules. An NBO analysis of the bonding in H(*x*im$^{Bu^t}$) derivatives demonstrates that the doubly bonded C═E resonance structure is most significant for the oxygen derivative, whereas singly bonded $C^+{-}E^-$ resonance structures dominate for the tellurium derivative. Although the latter result may appear counterintuitive because it is opposite to the trend that one would expect on the basis of electronegativity differences, it is precedented by studies on XC(E)NH_2 derivatives. In this regard, the C−E bonding in these compounds is significantly different from that in chalcogenoformaldehyde derivatives for which the bonding is well represented by a $H_2C{=}E$ double bonded resonance structure. Finally, comparison of the C−E bond lengths of the imidazolechalcogenones with those of C−E single bonds indicates that the C−O bonds are anomalously short. This observation may be rationalized in terms of the oxygen derivative having not only the most significant π−component, but also a significant ionic component. The large ionic component for the C−O bond is a consequence of the σ- and π-bonds being polarized in the same direction. In contrast, the σ-polarization for the heavier chalcogens opposes the π-polarization, thereby reducing the negative charge on the chalcogen that is implied by the zwitterionic $C^+{-}E^-$ contribution, despite the fact that this contribution increases as the chalcogen becomes heavier.

■ EXPERIMENTAL SECTION

General Considerations. 1-*t*-Butylimidazol-2-one,[26] 1-methylbenzimidazol-2-one,[27] 1-*t*-butylbenzimidazol-2-one,[28a] and 1-t-butylbenzimidazole-2-thione[29a] were synthesized according to literature methods, and crystals suitable for X-ray diffraction were obtained by crystallization from solutions in CH_2Cl_2.

X-ray Structure Determinations. Single crystal X-ray diffraction data were collected on a Bruker Apex II diffractometer, and crystal data, data collection, and refinement parameters are summarized in Table 10. The structures were solved using direct methods and standard difference map techniques, and were refined by full-matrix least-squares procedures on F^2 with SHELXTL (Version 2008/4).[50]

Computational Details. Calculations were carried out using DFT as implemented in the Jaguar 7.6 (release 110) suite of ab initio quantum chemistry programs.[51] Geometry optimizations were performed with the B3LYP density functional[52] using the 6-31G** (C, H, N, O, S) and LAV3P (Se, Te) basis sets.[53] The energies of the optimized structures were reevaluated by additional single point calculations on each optimized geometry using cc-pVTZ(-f) correlation consistent triple-ζ (C, H, N, O, S) and LAV3P (Se, Te) basis sets. NBO and NRT calculations were performed with NBO 5.0[54] as implemented in the Jaguar suite of programs using the 6-31G** and LAV3P basis sets.

■ ASSOCIATED CONTENT

Ⓢ Supporting Information

CIF files and Cartesian coordinates for geometry optimized structures. This material is available free of charge *via* the Internet at http://pubs.acs.org.

■ AUTHOR INFORMATION

Corresponding Author

*E-mail: parkin@columbia.edu.

Notes

The authors declare no competing financial interest.

■ ACKNOWLEDGMENTS

We thank the National Science Foundation (CHE-1058987) for support of this research and for the REU program at Columbia (B. K.). A.A.-H. thanks the Government of Saudi Arabia for a scholarship. Dr. Joshua H. Palmer is thanked for providing Cartesian coordinates of the tautomers of H(sebenzim^R) and Professor Clark Landis is thanked for helpful discussions concerning the NBO analyses.

■ REFERENCES

(1) (a) Zav'yalov, S. I.; Ezhova, G. I.; Kravchenko, N. E.; Kulikova, L. B.; Dorofeeva, O. V.; Rumyantseva, E. E.; Zavozin, A. G. *Pharm. Chem. J.* **2004**, *38*, 256−260. (b) Wong, O.; Tsuzuki, N.; Richardson, M.; Rytting, H.; Konishi, R.; Higuchi, T. *Heterocycles* **1987**, *26*, 3153−3158.

(2) (a) Abramov, N. D.; Trzhtsinskaya, B. V. *Chem. Heterocycl. Compd.* **1988**, *24*, 1309−1321. (b) Kister, J.; Assef, G.; Mille, G.; Metzger, J. *Can. J. Chem.* **1979**, *57*, 813−821. (c) Van Lommen, G.; Doyon, J.; Coesemans, E.; Boeckx, S.; Cools, M.; Buntinx, M.; Hermans, B.; VanWauwe, J. *Bioorg. Med. Chem. Lett.* **2005**, *15*, 497−500. (d) Kruse, L. I.; Kaiser, C.; DeWolf, W. E., Jr.; Frazee, J. S.; Ross, S. T.; Wawro, J.; Wise, M.; Flaim, K. E.; Sawyer, J. L.; Erickson, R. W.; Ezekiel, M.; Ohlstein, E. H.; Berkowitz, B. A. *J. Med. Chem.* **1987**, *30*, 486−494. (e) Wolfe, D. M.; Schreiner, P. R. *Synthesis* **2007**, 2002−2008. (f) Laufer, S.; Wagner, G.; Kotschenreuther, D. *Angew. Chem., Int. Ed.* **2002**, *41*, 2290−2293. (g) Phillips, B. T.; Claremon, D. A.; Varga, S. L. *Synthesis* **1990**, 761−763.

(3) (a) Guziec, L. J.; Guziec, F. S., Jr. *J. Org. Chem.* **1994**, *59*, 4691−4692. (b) Taurog, A.; Dorris, M. L.; Guziec, L. J.; Guziec, F. S., Jr. *Biochem. Pharmacol.* **1994**, *48*, 1447−1453. (c) Roy, G.; Mugesh, G. *J. Am. Chem. Soc.* **2005**, *127*, 15207−15217. (d) Roy, G.; Das, D.; Mugesh, G. *Inorg. Chim. Acta* **2007**, *360*, 303−316. (e) Cristiani, F.; Devillanova, F. A.; Diaz, A.; Verani, G. *Phos. Sulf. Rel. Elem.* **1984**, *20*, 231−240. (f) Cristiani, F.; Devillanova, F. A.; Diaz, A.; Verani, G. *J. Chem. Soc., Perkin Trans. 2* **1984**, 1383−1386. (g) Mammadova, G. Z.; Matsulevich, Z. V.; Osmanov, V. K.; Borisov, A. V.; Khrustalev, V. N. *Acta Crystallogr.* **2012**, *E68*, o1381.

(4) (a) Landry, V. K.; Minoura, M.; Pang, K.; Buccella, D.; Kelly, B. V.; Parkin, G. *J. Am. Chem. Soc.* **2006**, *128*, 12490−12497. (b) Palmer, J. H.; Parkin, G. *Polyhedron* **2013**, *52*, 658−668.

(5) 1,3-Dialkyl-2-imidazolechalcogenone and saturated imidazolidine-2-chalcogenone compounds have also been investigated with respect to their use as ligands. See, for example: (a) Kimani, M. M.; Wang, H. C.; Brumaghim, J. L. *Dalton Trans.* **2012**, *41*, 5248−5259. (b) Arduengo, A. J., III; Davidson, F.; Dias, H. V. R.; Goerlich, J. R.; Khasnis, D.; Marshall, W. J.; Prakasha, T. K. *J. Am. Chem. Soc.* **1997**, *119*, 12742−12749. (c) Kim, H. R.; Jung, I. G.; Yoo, K.; Jang, K.; Lee, E. S.; Yun, J.; Son, S. U. *Chem. Commun.* **2010**, *46*, 758−760. (d) Williams, D. J.; Pennington, W. T.; VanDerveer, D.; Anderton, J. T.; White, K. M. *J. Chem. Crystallogr.* **2003**, *33*, 465−472. (e) Isab, A. A.; Wazeer, M. I. M.; Fettouhi, M.; Ahmad, S.; Ashraf, W. *Polyhedron* **2006**, *25*, 2629−2636. (f) Al-Amri, A. H. D.; Fettouhi, M.; Wazeer, M. I. M.; Isab, A. A. *Inorg. Chem. Commun.* **2005**, *8*, 1109−1112.

(6) While the compounds illustrated in Figure 1 are often commonly referred to as 2-imidazolones, 2-imidazolethiones, and 2-imidazoleselones (or imidazol-2-ones, imidazole-2-thiones, and imidazole-2-selones), their systematic names are 1-R-1,3-dihydro-2*H*-imidazol-2-one, 1-R-1,3-dihydro-2*H*-imidazole-2-thione and 1-R-1,3-dihydro-2*H*-imidazole-2-selone, respectively. However, it should be noted that these compounds have also been given a plethora of other names. For example, the most commonly encountered compound in this class, 1-methyl-1,3-dihydro-2*H*-imidazole-2-thione, is not only described by its trivial name, methimazole, but also by 1-methylimidazole-2-thione, 1-methylimidazole-2(3*H*)-thione, 1-methyl-3*H*-imidazole-2-thione, 1-methyl-1*H*-imidazole-2(3*H*)-thione, 3-methyl-imidazole-2-thione and 1-methyl-4-imidazoline-2-thione. In addition, methimazole has also been given names that actually correspond to its tautomer, e.g., 1-methyl-1*H*-imidazole-2-thiol, 1-methyl-2-mercapto-1*H*-imidazole, 2-mercapto-1-methyl-1*H*-imidazole, and mercapto-1-methylimidazole. For brevity, we refer to the compounds described herein as 2-imidazolones, 2-imidazolethiones and 2-imidazoleselones.

(7) The term "chalcogenone" is simply used to describe the presence of a CE functional group and is not intended to convey any distinction between C═E and zwitterionic C^+−E^- resonance structures.

(8) For this reason, these compounds are also referred to in the literature by a variety of other names, e.g., mercaptoimidazoles and selenoimidazoles.

(9) (a) Minkin, V. I.; Garnovskii, A. D.; Elguero, J.; Katritzky, A. R.; Denisko, O. V. *Adv. Heterocycl. Chem.* **2000**, *76*, 157−323. (b) Shtefan, E. D.; Vvedenskii, V. Y. *Russ. Chem. Rev.* **1996**, *65*, 307−314. (c) Elguero, J.; Marzin, C.; Katritzky, A. R.; Linda, P. *Adv. Heterocycl. Chem.*, Suppl. *1* (1976).

(10) (a) Ren, Y.; Li, M.; Wong, N. B. *J. Mol. Model.* **2005**, *11*, 167−173. (b) Contreras, J. G.; Madariaga, S. T. *J. Phys. Org. Chem.* **2003**, *16*, 47−52. (c) Öğretir, C.; Yarligan, S. *J. Mol. Struct.* **1996**, *366*, 227−231.

(11) (a) Flakus, H. T.; Miros, A.; Jones, P. G. *Spectrochim. Acta Part A* **2002**, *58*, 225−237. (b) Vampa, G.; Benvenuti, S.; Severi, F.; Malmusi, L.; Antolini, L. *J. Heterocyclic Chem.* **1995**, *32*, 227−234. (c) Raper, E. S.; Creighton, J. R.; Oughtred, R. E.; Nowell, I. W. *Acta Crystallogr.* **1983**, *B39*, 355−360. (d) Balestrero, R. S.; Forkey, D. M.; Russell, J. G. *Magn. Reson. Chem.* **1986**, *24*, 651−655. (e) Garner, M.; Armstrong, D. R.; Reglinski, J.; Smith, W. E.; Wilson, R.; McKillop, J. H. *Bioorg. Med. Chem. Lett.* **1994**, *4*, 1357−1360. (f) Raper, E. S. *Coord. Chem. Rev.* **1985**, *61*, 115−184. (g) Form, G. R.; Raper, E. S.; Downie, T. C. *Acta Crystallogr.* **1976**, *B32*, 345−348. (h) Simanek, E. E.; Tsoi, A.; Wang, C. C. C.; Whitesides, G. M.; McBride, M. T.; Palmore, G. T. R. *Chem. Mater.* **1997**, *9*, 1954−1961. (i) McBride, M. T.; Luo, T. J. M.; Palmore, G. T. R. *Cryst. Growth Des.* **2001**, *1*, 39−46. (j) Zhu, H.-J.; Ren, Y.; Ren, J.; Chu, S.-Y. *J. Mol. Struct.* **2005**, *730*, 199−205. (k) Guo, Y.; Li, B. *Acta Chim. Sin.* **2007**, *65*, 1561−1567. (l) Bojarska-Olejnik, E.; Stefaniak, L.; Witanowski, M.; Hamdi, B. T.; Webb, G. A. *Magn. Reson. Chem.* **1985**, *23*, 166−169.

(12) (a) Devor, D. C.; Singh, A. K.; Frizzell, R. A.; Bridges, R. J. *Am. J. Physiol. (Lung Cell. Mol. Physiol.)* **1996**, *271*, L775−L784. (b) Devor, D. C.; Singh, A. K.; Bridges, R. J.; Frizzell, R. A. *Am. J. Physiol. (Lung Cell. Mol. Physiol.)* **1996**, *271*, L785−L795. (c) Kusama, N.; Kajikuri, J.; Yamamoto, T.; Watanabe, Y.; Suzuki, Y.; Katsuya, H.; Itoh, T. *Br. J. Pharmacol.* **2005**, *146*, 487−497. (d) Adeagbo, A. O. S. *Eur. J. Pharmacol.* **1999**, *379*, 151−159. (e) Anderson, N. J.; Slough, S.; Watson, W. P. *Eur. J. Pharmacol.* **2006**, *546*, 48−53. (f) Garduno, J.; Galvan, E.; de Sevilla, D. F.; Buno, W. *Neuropharmacology* **2005**, *49*, 376−388. (g) Large, C. H.; Terstappen, G. C. US Patent #0029773 A1, 2004. (h) Bezensek, J.; Groselj, U.; Stare, K.; Svete, J.; Stanovnik, B. *Tetrahedron* **2012**, *68*, 516−522. (i) Dandepally, S. R.; Williams, A. L. *Tetrahedron Lett.* **2009**, *50*, 1395−1398.

(13) (a) Cooper, D. S. *New Engl. J Med.* **2005**, *352*, 905−917. (b) Fumarola, A.; Di Fiore, A.; Dainelli, M.; Grani, G.; Calvanese, A. *Exp. Clin. Endocrinol. Diabet.* **2010**, *118*, 678−684.

(14) (a) Roy, G.; Mugesh, G. *Phosphorus Sulfur Silicon Relat. Elem.* **2008**, *183*, 908−923. (b) Roy, G.; Mugesh, G. *Chem. Biodivers.* **2008**, *5*, 414−439. (c) Roy, G.; Bhabak, K. P.; Mugesh, G. *Crys. Growth Des.* **2011**, *11*, 2279−2286. (d) Roy, G.; Mugesh, G. *Bioinorg. Chem. Appl.* **2006**, 1−9. (e) Roy, G.; Mugesh, G. *J. Chem. Sci.* **2006**, *118*, 619−625.

(15) Yamashita, Y.; Yamashita, M. *J. Biol. Chem.* **2010**, *285*, 18134−18138.

(16) Hu, Y.-C.; Liang, C.-F.; Tsai, J.-H.; Yap, G. P. A.; Chang, Y.-T.; Ong, T.-G. *Organometallics* **2010**, *29*, 3357−3361.

(17) (a) White, J. L.; Tanski, J. M.; Churchill, D. G.; Rheingold, A. L.; Rabinovich, D. *J. Chem. Crystallogr.* **2003**, *33*, 437−445. (b) Pang, K.; Figueroa, J. S.; Tonks, I. A.; Sattler, W.; Parkin, G. *Inorg. Chim. Acta* **2009**, *362*, 4609−4615. (c) Cingolani, A.; Effendy; Marchetti, F.; Pettinari, C.; Pettinari, R.; Skelton, B. W.; White, A. H. *Inorg. Chem.* **2002**, *41*, 1151−1161. (d) Fisher, M. G.; Gale, P. A.; Light, M. E.; Quesada, R. *CrystEngComm* **2008**, *10*, 1180−1190. (e) Aggarwal, V.; Kumar, V. R.; Singh, U. P. *J. Chem. Crystallogr.* **2011**, *41*, 121−126.

(f) Norris, A. R.; Taylor, S. E.; Buncel, E.; Bélanger-Gariépy, F.; Beauchamp, A. L. *Can. J. Chem.* **1983**, *61*, 1536−1541. (g) Bell, N. A.; Branston, T. N.; Clegg, W.; Creighton, J. R.; Cucurull-Sánchez, L.; Elsegood, M. R. J.; Raper, E. S. *Inorg. Chim. Acta* **2000**, *303*, 220−227. (h) Sultana, R.; Lobana, T. S.; Sharma, R.; Castineiras, A.; Akitsu, T.; Yahagi, K.; Aritake, Y. *Inorg. Chim. Acta* **2010**, *363*, 3432−3441. (i) Dodds, C. A.; Lehmann, M.-A.; Ojo, J. F.; Reglinski, J.; Spicer, M. D. *Inorg. Chem.* **2004**, *43*, 4927−4934. (j) Butler, L. M.; Creighton, J. R.; Oughtred, R. E.; Raper, E. S.; Nowell, I. W. *Inorg. Chim. Acta* **1983**, *75*, 149−154. (k) Oughtred, R. E.; Raper, E. S.; Nowell, I. W. *Inorg. Chim. Acta* **1984**, *84*, L5−L8. (l) Isaia, F.; Aragoni, M. C.; Arca, M.; Caltagirone, C.; Castellano, C.; Demartin, F.; Garau, A.; Lippolis, V.; Pintus, A. *Dalton Trans.* **2011**, *40*, 4505−4513. (m) Isaia, F.; Aragoni, M. C.; Arca, M.; Demartin, F.; Devillanova, F. A.; Floris, G.; Garau, A.; Hursthouse, M. B.; Lippolis, V.; Medda, R.; Oppo, F.; Pira, M.; Verani, G. *J. Med. Chem.* **2008**, *51*, 4050−4053. (n) Atkinson, E. R.; Gardiner, D. J.; Jackson, A. R. W.; Raper, E. S. *Inorg. Chim. Acta* **1985**, *98*, 35−41. (o) Ibrahim, M. M.; Shaban, S. Y. *Inorg. Chim. Acta* **2009**, *362*, 1471−1477. (p) Bristow, S.; Harrison, J. A.; Farrugia, L. J. *Polyhedron* **1987**, *6*, 2177−2180. (q) Docrat, A.; Morlok, M. M.; Bridgewater, B. M.; Churchill, D. G.; Parkin, G. *Polyhedron* **2004**, *23*, 481−488. (r) Morlok, M. M.; Docrat, A.; Janak, K. E.; Tanski, J. M.; Parkin, G. *Dalton Trans.* **2004**, 3448−3452. (s) Matsunaga, Y.; Fujisawa, K.; Amir, N.; Miyashita, Y.; Okamoto, K.-I. *J. Coord. Chem.* **2005**, *58*, 1047−1061.

(18) Melnick, J. G.; Yurkerwich, K.; Parkin, G. *Inorg. Chem.* **2009**, *48*, 6763−6772.

(19) Al-Harbi, A.; Sattler, W.; Sattler, A.; Parkin, G. *Chem. Commun.* **2011**, *47*, 3123−3125.

(20) Garner, M.; Reglinski, J.; Cassidy, I.; Spicer, M. D.; Kennedy, A. R. *Chem. Commun.* **1996**, 1975−1976.

(21) (a) Spicer, M. D.; Reglinski, J. *Eur. J. Inorg. Chem.* **2009**, 1553−1574. (b) Parkin, G. *New J. Chem.* **2007**, *31*, 1996−2014. (c) Smith, J. M. *Comments Inorg. Chem.* **2008**, *29*, 189−233.

(22) Minoura, M.; Landry, V. K.; Melnick, J. G.; Pang, K.; Marchiò, L.; Parkin, G. *Chem. Commun.* **2006**, 3990−3992.

(23) Landry, V. K.; Pang, K.; Quan, S. M.; Parkin, G. *Dalton Trans.* **2007**, 820−824.

(24) Bis(2-mercaptoimidazolyl)hydroborato and bis(2-selenoimidazolyl)hydroborato ligands are also known. See, for example: (a) Kimblin, C.; Bridgewater, B. M.; Hascall, T.; Parkin, G. *J. Chem. Soc., Dalton Trans.* **2000**, 891−897. (b) Kimblin, C.; Hascall, T.; Parkin, G. *Inorg. Chem.* **1997**, *36*, 5680−5681. (c) Landry, V. K.; Buccella, D.; Pang, K.; Parkin, G. *Dalton Trans.* **2007**, 866−870. (d) Landry, V. K.; Parkin, G. *Polyhedron* **2007**, *26*, 4751−4757.

(25) For some examples, see: (a) Belaziz, D.; Kandri Rodi, Y.; Essassi, E. M.; El Ammari, L. *Acta Crystallogr.* **2012**, *E68*, o1276. (b) Ouzidan, Y.; Essassi, E. M.; Luis, S. V.; Bolte, M.; El Ammari, L. *Acta Crystallogr.* **2011**, *E67*, o1822. (c) Saber, A.; Zouihri, H.; Essassi, E. M.; Ng, S. W. *Acta Crystallogr.* **2010**, *E66*, o1409. (d) Cui, D.; Li, Y.; Lian, M.; Yang, F.; Meng, Q. *Analyst* **2011**, *136*, 3149−3156.

(26) Quast, H.; Nahr, U. *Chem. Ber.* **1984**, *117*, 2761−2778.

(27) Prakash, O.; Batra, H.; Kaur, H.; Sharma, P. K.; Sharma, V.; Singh, S. P.; Moriarty, R. M. *Synthesis* **2001**, 541−543.

(28) (a) Zhang, P.; Terefenko, E. A.; Bray, J.; Deecher, D.; Fensome, A.; Harrison, J.; Kim, C.; Koury, E.; Mark, L.; McComas, C. C.; Mugford, C. A.; Trybulski, E. J.; Vu, A. T.; Whiteside, G. T.; Mahaney, P. E. *J. Med. Chem.* **2009**, *52*, 5703−5711. (b) Olofson, R. A.; Vandermeer, R. K.; Hoskin, D. H.; Bernheim, M. Y.; Stournas, S.; Morrison, D. S. *J. Org. Chem.* **1984**, *49*, 3367−3372.

(29) (a) Ellsworth, E. L.; Domagala, J.; Prasad, J. V. N.V; Hagen, S.; Ferguson, D.; Holler, T.; Hupe, D.; Graham, N.; Nouhan, C.; Tummino, P. J.; Zeikus, G.; Lunney, E. A. *Bioorg. Med. Chem. Lett.* **1999**, *9*, 2019−2024. (b) Kawauchi, I. U. S. Patent 2008/0081291 A1. (c) Bäuerlein, E.; Trasch, H. *Liebigs Ann. Chem.* **1979**, 1818−1827.

(30) See, for example, refs 17a 11b, c, g, i, and (a) Steiner, T. *Angew. Chem., Int. Ed.* **2002**, *41*, 48−76. (b) Allen, F. H.; Bird, C. M.; Rowland, R. S.; Raithby, P. R. *Acta Crystallogr.* **1997**, *B53*, 696−701. (c) Allen, F. H.; Bird, C. M.; Rowland, R. S.; Raithby, P. R. *Acta Crystallogr.* **1997**, *B53*, 680−695.

(31) Khan, H.; Badshah, A.; Shaheen, F.; Gieck, C.; Qureshi, R. A. *Acta Crystallogr.* **2008**, *E64*, o1141.

(32) Cambridge Structural Database (Version 5.34). *3D Search and Research Using the Cambridge Structural Database* Allen, F. H.; Kennard, O. *Chemical Design Automation News* **1993**, *8* (1), pp 1 and 31−37.

(33) The C$^+$−E$^-$ abbreviation is being used simply to convey any resonance structure that has a C−E single bond and not specifically one in which the formal positive charge is localized on carbon.

(34) For a discussion of the most appropriate Lewis structures in representing molecules, see: Suidan, L.; Badenhoop, J. K.; Glendening, E. D.; Weinhold, F. *J. Chem. Educ.* **1995**, *72*, 583−586.

(35) Weinhold, F.; Landis, C. R. *Valency and Bonding: A Natural Bond Orbital Donor-Acceptor Perspective*; Cambridge University Press: New York, 2005.

(36) For studies which discuss the fact that transition metal oxo bond lengths are also exceptionally short, see: (a) Howard, W. A.; Parkin, G. *J. Am. Chem. Soc.* **1994**, *116*, 606−615. (b) Parkin, G. *Prog. Inorg. Chem.* **1998**, *47*, 1−165. (c) Trnka, T. M.; Parkin, G. *Polyhedron* **1997**, *16*, 1031−1045.

(37) (a) Glendening, E. D.; Landis, C. R.; Weinhold, F. *WIREs Comput. Mol. Sci.* **2012**, *2*, 1−42. (b) Weinhold, F. *J. Comput. Chem.* **2012**, *33*, 2363−2379.

(38) The contribution of zwitterionic resonance structures has also been reported to be more significant for the heavier chalcogen in six-membered heterocyclic compounds. See, for example: Mautner, H. G.; Chu, S.-H.; Lee, C. M. *J. Org. Chem.* **1962**, *27*, 3671−3673.

(39) For related studies on H$_2$CO, H$_2$CS, and H$_2$CSe, see ref 35.

(40) It has previously been noted that the σ and π electrons may exhibit opposite polarizations to minimize electron repulsion. See ref 43.

(41) Glendening, E. D.; Hrabal, J. A., II *J. Am. Chem. Soc.* **1997**, *119*, 12940−12946.

(42) Note that zwitterionic resonance structures in which the positive formal charge is localized on carbon contribute very little to the overall bonding because of the availability of lone pairs on the adjacent nitrogen atoms. As such, the formal positive charge of the zwitterionic structures is more appropriately localized on the nitrogen atoms.

(43) (a) Moudgil, R.; Bharatam, P. V.; Kaur, R.; Kaur, D. *Proc. Indian Acad. Sci. (Chem. Sci.)* **2002**, *114*, 223−230. (b) Bharatam, P. V.; Moudgil, R.; Kaur, D. *J. Phys. Chem. A* **2003**, *107*, 1627−1634.

(44) Wiberg, K. B. *Acc. Chem. Res.* **1999**, *32*, 922−929.

(45) Mo, Y.; Schleyer, P. v. R.; Wu, W.; Lin, M.; Zhang, Q.; Gao, J. *J. Phys. Chem. A* **2003**, *107*, 10011−10018.

(46) Lauvergnat, D.; Hiberty, P. C. *J. Am. Chem. Soc.* **1997**, *119*, 9478−9482.

(47) (a) Kaur, D.; Sharma, P.; Bharatam, P. V.; Dogra, N. *J. Mol. Struct.: Theochem.* **2006**, *759*, 41−49. (b) Kaur, D.; Sharma, P.; Bharatam, P. V. *J. Mol. Struct.: Theochem.* **2005**, *757*, 149−153.

(48) Huang, Y.; Jahreis, G.; Fischer, G.; Lücke, C. *Chem.—Eur. J.* **2012**, *18*, 9841−9848.

(49) It has also been suggested that the greater polarisability of the heavier chalcogen allows it to accommodate a greater charge. See ref 41.

(50) (a) Sheldrick, G. M. SHELXTL, An Integrated System for Solving, Refining and Displaying Crystal Structures from Diffraction Data; University of Göttingen, Göttingen, Federal Republic of Germany, 1981. (b) Sheldrick, G. M. *Acta Crystallogr.* **2008**, *A64*, 112−122.

(51) *Jaguar 7.6*; Schrödinger, LLC: New York, NY, 2009.

(52) (a) Becke, A. D. *J. Chem. Phys.* **1993**, *98*, 5648−5652. (b) Becke, A. D. *Phys. Rev. A* **1988**, *38*, 3098−3100. (c) Lee, C. T.; Yang, W.; Parr, R. G. *Phys. Rev. B* **1988**, *37*, 785−789. (d) Vosko, S. H.; Wilk, L.; Nusair, M. *Can. J. Phys.* **1980**, *58*, 1200−1211. (e) Slater, J. C. Quantum Theory of Molecules and Solids, Vol. *4*. *The Self-Consistent Field for Molecules and Solids*; McGraw-Hill: New York, 1974.

(53) (a) Hay, P. J.; Wadt, W. R. *J. Chem. Phys.* **1985**, *82*, 270−283. (b) Wadt, W. R.; Hay, P. J. *J. Chem. Phys.* **1985**, *82*, 284−298. (c) Hay, P. J.; Wadt, W. R. *J. Chem. Phys.* **1985**, *82*, 299−310.

(54) Glendening, E. D.; Badenhoop, J. K.; Reed, A. E.; Carpenter, J. E.; Bohmann, J. A.; Morales, C. M.; Weinhold, F. Theoretical Chemistry Institute, University of Wisconsin: Madison, WI, 2001; http://www.chem.wisc.edu/~nbo5.